

Fluid-Structure Interaction Modeling of Aortic Valve Stenosis at Different Heart Rates

Hamidreza Ghasemi Bahraseman^{1*}, Ehsan Mohseni Languri¹, Niloofar Yahyapourjalaly², Daniel M. Espino³

¹Department of Mechanical Engineering, Tennessee Technological University, Cookeville, USA

²Johns Hopkins Hospital, Baltimore, USA

³School of Mechanical Engineering, University of Birmingham, Birmingham, England, UK

*Corresponding Author:

Hamidreza Ghasemi Bahraseman, 1Department of Mechanical Engineering, Tennessee Technological University, 1 William L Jones Dr, 38501 Cookeville, TN, Cookeville, USA, Tel: (901) 567-8750, e-mail: hghasemib42@students.tntech.edu

Abstract

Purpose: This paper proposes a model to measure the cardiac output and stroke volume at different aortic stenosis severities using a fluid-structure interaction (FSI) simulation at rest and during exercise.

Methods: The geometry of the aortic valve is generated using echocardiographic imaging. An Arbitrary Lagrangian-Eulerian mesh was generated in order to perform the FSI simulations. Pressure loads on ventricular and aortic sides were applied as boundary conditions.

Results: FSI modeling results for the increment rate of cardiac output and stroke volume to heart rate, were about 58.6% and -14%, respectively, at each different stenosis severity. The mean gradient of curves of cardiac output and stroke volume to stenosis severity were reduced by 57% and 48%, respectively, when stenosis severity varied from healthy to critical stenosis.

Conclusions: Results of this paper confirm the promising potential of computational modeling capabilities for clinical diagnosis and measurements to predict stenosed aortic valve parameters including cardiac output and stroke volume at different heart rates.

Keywords: aortic valve, cardiac output, stenosis, stroke volume, fluid-structure interaction

1. Introduction

It is undoubtedly true that cardiac disease still remains the principal cause of death worldwide, in spite of advances in prevention, diagnosis and even therapies [26]. Three percent of individuals 65 years and older are affected by aortic valve stenosis, the greatest morbidity of cardiac valve diseases [24]. Aortic valve stenosis causes cardiac output reduction as an explained failure of the heart [8]. Therefore, assessing aortic valve stenosis parameters and its effects on cardiac function is important for diagnosis of related diseases. Currently, invasive and non-invasive methods are typically used to detect aortic valve stenosis. Existing clinical methods to measure aortic valve stenosis including angiography, catheterization, magnetic resonance imaging (MRI), and ultrasound need the attainability of large scale and costly equipment [23] that involve difficulties and are associated with risks [23]. Since it is very challenging to assess required parameters for such diseases from a specified subject clinically, computational methods show promising potential to simulate and evaluate the aortic valve's function. This study focuses on the aortic stenosis severity and its effects on cardiac output and stroke volume using a finite element (FE) based fluid-structure interaction (FSI) method.

FSI simulations are well suited to heart valve modeling due to concurrent prediction of structural deformation and hemodynamics. Bahraseman *et al.* [2], [3] have previously predicted cardiac output and stroke volume for a healthy subject by coupling Echo-Doppler measurements with FSI models during exercise and used this combination to predict hemodynamics [2]. There have been recent studies on applying FSI modeling techniques to cardiovascular applications [11]. For concurrent FSI at fluid-solid interface boundaries, the fluid velocity is equal to the structural time-dependent deformation and the forces on the solid are induced through flow conditions [11-32]. Donea *et al.* [10] used an Arbitrary-Lagrange-Euler (ALE) mesh to discretize governing equations in their transient FSI modeling. According to the presented literature review, there is limited application of FSI to study aortic valve disease and its progression [15]. It can be crucial and helpful to clinicians if the effects of parameters such as heart rate (e.g., due to exercise) on the performance of aortic valve with stenosis assessed numerically.

In this study, the cardiac output and stroke volume have been investigated numerically during exercise in the presence of aortic stenosis. A two-dimensional FSI simulation has been applied. Different severities of aortic valve stenosis have been considered and classified as: Healthy, Normal, Mild, Moderate, Severe and Critical. For each condition, the distance between leaflet tips was specified in the simulation. The boundary conditions were considered based on the calculation of brachial pressures and also the changes in brachial, Aortic and left ventricular pressures. The model represented a natural aortic valve as the increasing systolic pressure initiated valve opening and, sequentially, blood flow was ejected through the aorta artery. As ventricular systolic pressure lowered, when systole is ended, the aortic valve closes. Combining non-invasive pressure measurements with the FSI modeling results in calculation of cardiac output and stroke volume depending on different severities. The two-dimensional model geometry was acquired by Echo-Doppler and boundary conditions were calculated from measurements on a subject. Consequently, these estimations were specific to the subject. Material properties were taken from the literature due to non-availability in a clinical setting. Model verification was carried out by comparing numerical results to measurements from echocardiography (ECG).

2. Material and Methods

2.1 Overview

Figure 1 demonstrates the current study's workflow for numerical simulation and validation. The authors have previously explained and validated the subject-specific 2D FSI model in depth [3]. A brief overview of the model combined with clinical procedure is presented here.

2.2 Combined clinical and numerical approach

Hemodynamic data recorded during rest and exercise for a 33 year old healthy male, with normal cardiovascular function with his informed consent, was obtained according to protocols approved ethically by the Department of Cardiovascular Imaging (Atherosclerosis research center, Tehran, Iran). The volunteer was found to have normal cardiovascular performance during the physical examination. This was determined from bicycle exercise exams and Doppler ECG. Systolic and diastolic pressures of the brachial artery were measured at different heart rates (Fig. 2). The Mean Arterial pressure was calculated based on the Equation 1 [29]:

$$\text{MAP} = \text{DBP} + \left(\frac{1}{3} + 0.0012\text{HR}\right) \cdot (\text{SBP} - \text{DBP}) \quad (1)$$

where MAP is the Mean Arterial Pressure, DBP the Diastolic Blood Pressure and SBP the Systolic Blood Pressure. Moreover, an increased valve stiffness leads toward smaller orifice areas as well as a greater pressure drop across valves [29].

Equations 2 and 3 are applied to calculate the Aortic pressure from brachial pressure [27]. Park et al. [27] obtained these relations by comparing brachial pressure (acquired by Oscillometry) to the Aortic pressure acquired using an invasive method.

$$\text{Aortic systolic pressure} \approx \text{Brachial systolic pressure} + 2.25 \quad (2)$$

$$\text{Aortic diastolic pressure} \approx \text{Brachial diastolic pressure} - 5.45 \quad (3)$$

where all pressures were measured in *mmHg*. The difference between left ventricular systolic pressure to aortic systolic pressure was assumed to be *5 mmHg on average*. This was obtained by solving the full Navier-Stokes equation (i.e. accounting for convective, transient and viscous components [22]).

The computer aided design (CAD) model of the aortic valve employed in the FSI modeling of this paper is presented in Fig. 3 and its dimensions are provided in Table 1. Utilizing the resting para-sternal long-axis view, dimensions were shown based on T-wave (The T wave represents the repolarization of the ventricles) of ECG at the peak T-wave time (maximum opening area). The two cusps have been considered as homogenous, isotropic, and to have a linear stress-strain behavior [13], [14]. Moreover, blood is assumed to be an incompressible and Newtonian fluid [5]. Properties of the blood are presented in Table 2 [17], [20].

The Dirichlet pressure boundary condition was applied to the inflow boundary of the aortic root at the left ventricular side (Fig. 3). Furthermore, second order Lagrangian elements were applied for the mesh generation with a total of 7001 elements. The Comsol Multi-Physics 4.3 solver was employed to solve the time-dependent FSI model using finite element analysis [12], [13].

2.3 Stenosis Simulation

The bowl-shaped leaflets of the natural aortic valve prevent the valve from excessive opening under high physical pressure [30]. A virtual spring was used in the form of Equation 4 to impede excessive opening in our two-dimensional model [7]:

$$f_s = -k \cdot (d - d_0) \quad (4)$$

In Equation 4, f_s is force, d is the displacement and k is a diagonal stiffness matrix. The k value in the modeling was given a large value (10^9) to effectively prevent excessive opening. The term d_0 , is an optional pre-deformation that was regarded as zero in this situation. This is owing to the spring foundations being connected to the leaflets when the leaflets tip position is at its peak. And at this time pre-deformation is equal to zero. Aortic valve stenosis severity was classified as either Normal, Mild, Moderate, Severe or Critical (Table 3). Using data from literature [4], the relationship between the aortic valve's orifice radius and stenosis severity was derived. These radii are provided in Table 3. Stenosis was modelled as a restriction of the maximum opening radius. For each stenosis severity, the aortic valve opened up to its corresponding orifice radius. This was achieved by using the virtual spring (Equation 3). Due to the spring's large stiffness value, it provides an exact radius of openings for each severity of stenosis. Subsequently, all stenosed orifice radii were confirmed during post-processing. The aortic valve radius was considered a constant for each severity of stenosis across all the heart

rates of the simulation. The process is pretty similar to gap functions used for contact modelling, with the difference that in contact modelling you use the force to prevent ‘penetration’, whereas here we don’t want to exceed a certain separation distance.

ACCEPTED

3. Results

3.1 Cardiac output changes at various severities of stenosis

The cardiac output values at different heart rates are demonstrated in Fig. 4 where different stenosis stages are considered during rest and exercise. As provided in Table 3 and Fig. 4, the increase in cardiac output owing to exercise shows a moderate decline when the stenosis severity is increased. This increment fluctuates from 58.4% to 60.0%, with an average value of 58.9%.

3.2 Stroke volume changes at various severities of stenosis

The amount of overall decrease in stroke volume owing to exercise shows a moderate increase when the stenosis severity is increased, Fig. 5. This value fluctuates from 7.1% to 9.0% with an average value of 8.3%, Table 3.

3.3 Cardiac output changes to heart rate at different stenosis severities

The mean gradient of cardiac output to heart rate shows a noticeable decrease as the stenosis severity increased (Fig. 6). As provided in Table 4, this gradient changed from -36 to -83 $ml/min \cdot bpm$, and its mean value is -56 $ml/min \cdot bpm$.

3.4 Stroke volume changes with heart rate at different stenosis severities

Figure 7 shows that absolute amount of mean slope of stroke volume changes with heart rate with a decrease when the stenosis severity is increased. This value changes from -0.052 to -0.100 $ml/beat.bpm$, and its mean value is -0.077 $ml/beat.bpm$, Table 3. As provided in Table 4 and (Fig. 4), the absolute amount of mean slope of cardiac output changes to stenosis severity shows a significant increase when the heart rate is increased. This value changes from -91 to -147 ml/min , and its mean value is -122 ml/min . The change in stroke volume changes with stenosis severity shows a moderate decrease when the heart rate is increased (Table 3 and Fig. 5). This value changes from -0.92 to -0.87 $ml/beat$, and its mean value is -0.91 $ml/beat$.

3.5 Cardiac output changes to mean arterial pressure at different stenosis severities

The cardiac output values at different mean arterial pressures are demonstrated in Fig. 8 where different stenosis stages are considered during rest and exercise. As provided in Table 3 and Fig. 8, the cardiac output is increased for all stenosis severities when the mean arterial pressure is increased. The mean slope of cardiac output changes to mean arterial pressure ($ml/min.mmHg$) shows a noticeable decrease as the stenosis severity is increased, Table 3. This value changed from -19.7 to -8.5($ml/min.mmHg$).

3.6 Stroke volume changes to mean arterial pressure at different stenosis severities

Figure 9 shows the stroke volume values at different mean arterial pressures considering various stenosis stages during rest and exercise. As provided in Table 3 and Fig. 9, the stroke volume is slightly decreased for all stenosis severities when the mean arterial pressure is increased. The mean slope of stroke volume changes to mean arterial pressure shows a decrease as the stenosis severity increased, Table 3. This changed from -0.42 to -0.22 ($ml/beat.mmHg$).

ACCEPTED

4. Discussion

4.1 Study findings

FSI modeling is employed to predict changes in cardiac output and stroke volume during exercise through a stenosed aortic valve. To the best of authors' knowledge, it is the first time that an FSI simulation tool is utilized to obtain a numerical estimation of a stenosed aortic valve during exercise. The simulation's results predict that with increasing heart rate during the left ventricular ejection phase:

- Cardiac output ranged from 58.4% to 60% regardless of stenosis severity.
- Stroke volume decreases by 14% from a healthy condition to critical severity of stenosis;
- The mean gradient of cardiac output changes to stenosis severity decreases by 57% from healthy to critical severity of stenosis;
- The mean gradient of stroke volume changes to stenosis severity decreases by 48% from healthy to critical severity of stenosis.

The results of the subject specific 2D fluid–structure interaction model have been validated against clinical data measured from a volunteer [3]. The parameters obtained reliably for the subject through clinical measurements were reported. Hence, the predicted mean velocity, cardiac output and stroke volume were validated against the respective Echo-Doppler results, under conditions of increasing exercise. The current study presents a simplified model that estimates cardiovascular performance at disease stages for a wide range of time-dependent and variable boundary conditions, including different severities of aortic stenosis and increasing heart rates.

4.2 Clinical application and reliability

It has been proven that Catheterization-Thermodilution is the golden standard to evaluate cardiac performance like cardiac output and stroke volume [23]. Yet, it is associated with risks including cardiac arrhythmia, heart failure, and even death due to its invasive method [23]. Moreover, the patient and physician are probably exposed to damaging radiation by Thermodilution [23]. Exercising while catheterization is not common practice because of a range of technical problems. However, non-invasive measurements of patient cardiac function during an exercise protocol are possible by using numerical simulation [2].

Numerical simulation also predicts cardiac output without limitations associated with inter- and intra-observer variability associated with Echo-Doppler for stenosed aortic valves. Additionally, personal expertise and the image capture ability of the echocardiologists do not influence results from numerical simulations [3]. Therefore, the credibility of numerical methods to predict cardiac output and stroke volume is maintained. Our FSI model validation was performed using clinical measurements [3] for the self-same subject from which the model parameters were obtained. Hence, the results of applying the stenosis to the model are reliable.

The presented numerical approach would also be capable of predicting the severity of stenosis by recording the cardiac outputs of subject at two or three different heart rates and calculating the mean gradient of cardiac output to the specific heart rate.

Predicting the effect of aortic stenosis severity on cardiac function is vital in assessing stenosis severity progression. Furthermore, such predictions would equip physicians to estimate the disease progress. Moreover, the effect of increasing heart rate (e.g. due to exercise) on the cardiac function at different stenosis severities can be predicted. However, the non-invasive method of our study as well as merits of being frugal and simple, mean this method would avoid current invasive and very costly techniques associated with some risks for both patient and physician. This should be noted that further clinical investigations are necessary to practically develop our proposed model.

The curves in Fig. 4- Fig. 9 are interpolations of numerical results at different heart rates or different stenosis severities. Our numerical results are validated with literature using the healthy stage. This study demonstrates that it is feasible to make very specific predictions of changes in hemodynamics if aortic stenosis were to develop/worsen for a subject. As shown in our second paper [2], this could be extended to include hemodynamics and leaflet stress. Potentially equipping clinicians with further information to aid their decision on when, or how best, to intervene with progressive stenosis on a patient by patient basis.

4.3 Comparison to literature

To the best of the authors' knowledge, there are no published numerical results to compare the cardiac function over the different severities of stenosis during exercise. In this paper, patient specific cardiac output was predicted at a range of heart rates induced by exercise. There are only

a few models available describing *in vitro* approaches for the stenosed aortic valve [16], [25], [28] which do not consider the exercise and stenosis stages parameters in their modeling. The hemodynamic behavior of the stenosed aortic valve is highly depending on severity of stenosis. There are several research studies that have been focused on treatment of stenosed aortic valve [18], [19]. Our results show that exercise (increasing in heart rate) did not influence the cardiac output over the different severity of stenosis. This is in agreement with the previous clinical research [1]. Bache *et al.* [1] clinically studied cardiac performance of 20 patients with the problem of stenosed aortic valves. They did not categorize their results in terms of the stenosis severity. They reported mean cardiac output of 5400 ml/min at a heart rate of 79 bpm for the whole subjects at rest stage. They also measured mean cardiac output of 8500 ml/min at heart rate of 112 bpm under exercise condition for all patients. Their findings qualitatively agree with our findings, however, further quantitative comparison would require a breakdown of their findings according to severity of stenosis.

4.4 Limitations & future trends

The main limitations of the current study are as follows.

1. Mechanical properties of both fluid and solid were simplified.
2. The single diameter of ascending area was considered constant.
3. The simulation was performed on a 2D model rather than a 3D model.
4. Statistical and generalized data were applied for clinical determination of hemodynamic parameters.
5. Park et al. [27] examined 84 patients who showed no significant stenosis and were negative for ergonovine provocation test. The patients consisted of 57 females and 27 males. They excluded the subjects with heart problems such as: brachial and central systolic pressure problems, significant valvular heart disease, significant cardiac arrhythmia and significant valvular heart disease. It should be noted that although measuring brachial pressure provides limitations in terms of determining aortic pressure, it has been found to be a valid approximation. Furthermore, it enables FSI models to use subject specific blood pressure leading to predictions specific for that individual. Based on Park et al. [27], the central systolic pressure can be estimated from brachial systolic pressure and observed biases seem to remain within the practical range. However, use of

the brachial diastolic pressure is doubtful in clinical practice because of their large biases [27]. We assumed their reported data for our simulation. For future research, central systolic and diastolic pressure could be measured for each patient specifically by the oscillometric method.

6. This study has ignored compliance of the aortic root, which could alter predictions related to a pressure drop across the valve. However, this is unlikely to alter the qualitative conclusions from this study following comparisons across stenosis grade. Further, there is experimental evidence suggesting that compliance of the aortic root does not have a major role in modulating pressure drops across the valve [9]. Using an *in vitro* experiments mock up with a compliant aortic root, with or without valve sinuses, De Paulis *et al.* [9] found that when the cardiac output was increased above 5 L/min, the pressure drop significantly increased only in the sample without sinuses.
7. Although homogenous stenosis is a simplification, a methodology to assess stenosis computationally is provided. The subsequent stage is to develop the model for site-specific stenosis. The orifice radius of aortic valve for each level of stenosis severity was derived based on that reported in the literature [4]. It was considered constant when heart rate was increased due to the exercise.
8. The assumption of rigid aortic walls was a model limitation which enabled a better simulation time (important clinically). This limitation might contribute to the model estimations being lower/higher than the real values measured. However, any bias introduced would likely remain constant across stenosis severity grades; thereby, not altering the conclusions from this study. Furthermore, in terms of effect of exercise and subsequently increased systolic pressure, Christie *et al.* [6] clinically studied and reported no considerable change in aortic diameter with exercise.

Despite the model limitations, some advantages were obtained including:

- Excellent agreement with clinical measurements and the general literature [3];
- The FSI model at the healthy stage has already led to a good cardiac output correlation with Doppler-derived values ($r = 0.999$), in addition a good correlation ($r = 0.94$) achieved for stroke volume [3];
- The short solution time for a 2D FSI model that can potentially be translated into clinical

applications. Moreover, the solution time can be enhanced with advance computer hardware;

- That variability can be included in the model and analyzed [21], while, a range of values for statistical comparison would not be predicted with experimental studies.

The ultimate rationale for calculating cardiac output in patients with aortic stenosis during exercise is to find relationship between cardiac output and stenosis severity at different stages. With further investigations with a larger number of subjects, useful subject specific (age, sex, etc.) information for physicians including cardiac output and the probable severity of stenosis can be calculated. Granted, echocardiography may not be perfectly accurate, but it is unlikely to be less accurate than a 2D FSI model, which involves many assumptions and simplifications. However, echocardiography alone does not have the capability to change boundary conditions and assess probable different situations.

5. Conclusion

We have performed two-dimensional fluid-structure interaction modeling of a stenosed aortic valve to predict cardiac output and stroke volume, during exercise. The numerical model is developed based on a subject specific case and solved through the finite element method. The results agree with the reported values in the literature. The method requires to be validated by more testing, including independent measurements of cardiac output and stroke volume. The benefit of using a two-dimensional simulation is the quick solution time, less than 15 minutes, can be utilized in clinical application.

Competing interests

Authors have declared that no competing interests exist.

Referemnces

- [1]. Bache R.J, Wang Y., Jorgensen C.R. Hemodynamic effects of exercise in isolated valvular aortic stenosis. *Circulation*. 1971, vol. 44(6), 1003-1013.
- [2]. Bahraseman H.G., Hassani K., Khosravi A., Navidbakhsh M., Espino D.M., Fatourae N., Kazemi-Saleh. Combining numerical and clinical methods to assess aortic valve hemodynamics during exercise. *Perfusion* 2014, vol. 29(4), 340-350.
- [3]. Bahraseman H.G., Hassani K., Navidbakhsh M., Espino D.M., Sani Z.A., Fatourae N. Effect of exercise on blood flow through the aortic valve: a combined clinical and numerical study. *Comput Methods Biomech Biomed Engin*. 2014, vol. 17(16), 1821-1834.
- [4]. Bonow R.O., Mann D.L., Zipes D.P., Libby P. *Braunwald's Heart Disease: A Textbook of Cardiovascular Medicine*. 9th ed. Philadelphia, Pa: Saunders Elsevier. 2011.
- [5]. Caro C.G., Pedley T.J., Schroter R.C., Seed W.A. *The mechanics of the circulation*. Oxford: Oxford University Press. 1978.
- [6]. Christie J., Sheldahl L.M., Tristani F.E., Sagar K.B., Ptacin M.J., Wann S. Determination of stroke volume and cardiac output during exercise: comparison of two-dimensional and Doppler echocardiography, Fick oximetry, and thermodilution. *Circulation*, 1987, vol. 76(3), 539-547.
- [7]. *Comsol Users Manual. Comsol Multiphysics Users Guide*. Londen: Comsol Ltd. 2011.

- [8]. Criner G.J., Barnette R.E., Alonzo G.E. *Critical Care Study Guide: Text and Review*. New York: Springer. 2010.
- [9]. De Paulis R., Salica A., Pisani G., Morbiducci U., Weltert L., Maselli D. Hemodynamics of the aortic valve and root: implications for surgery. *Ann Cardiothorac Surg*, 1987, vol. 2(1), 40.
- [10]. Donea J., Giuliani S., Halleux J.P. An arbitrary Lagrangian–Eulerian finite element method for transient dynamic fluid–structure interactions. *Comput Methods Appl Mech Eng*, 1982, vol. 33(1-3), 689–723.
- [11]. Dowell E.H., Hall K.C. Modelling of fluid-structure interaction. *Annu Rev Fluid Mech*. 2001, vol. 33(1), 445-490.
- [12]. Espino D.M., Shepherd D.E.T., Hukins D.W.L. A simple method for contact modelling in an arbitrary frame of reference within multi-physics software. *J Mech*, 2013, vol. 29(3), N9-N14.
- [13]. Espino D.M., Shepherd D.E.T., Hukins D.W.L. Development of a transient large strain contact method for biological heart valve simulations. *Comput Methods Biomech Biomed Engin*, 2013, vol. 16(4), 413-424.
- [14]. Espino D.M., Shepherd D.E.T., Hukins D.W.L. Evaluation of a transient, simultaneous, Arbitrary Lagrange Euler based multi-physics method for simulating the mitral heart valve. *Comput Methods Biomech Biomed Engin*, 2014, vol. 17(4), 450-458.
- [15]. Weinberg E.J., Kaazempur Mofrad M.R. A multiscale computational comparison of the bicuspid and tricuspid aortic valves in relation to calcific aortic stenosis. *J Biomech*, 2008, vol. 41(16), 3482-3487.
- [16]. Gould K., Carabello B. Why Angina in Aortic Stenosis With Normal Coronary Arteriograms? *Circulation*, 2003, vol. 107, 3121–3123.
- [17]. Govindarajan V., Udaykumar H.S, Herbertson L.H., Deutsch S., Manning K.B, Chandran K.B. Two-Dimensional FSI Simulation of Closing Dynamics of a Tilting Disk Mechanical Heart Valve. *J Med Devices*, 2010, vol. 4(1), 011001(1-11).
- [18]. Gurvitch R., Cheung A., Bedogni F., Webb J.G. Coronary obstruction following transcatheter aortic valve-in-valve implantation for failed surgical bioprostheses. *Catheter Cardiovasc Interv*. 2011, vol. 77(3), 445-446.

- [19]. Hammerstingl C., Nickenig G., Grube E. Treatment of a degenerative stenosed CoreValve® aortic bioprosthesis by transcatheter valve-in-valve insertion. *Catheter Cardiovasc Interv*, 2012, vol. 79(5), 748-755.
- [20]. Koch T.M., Reddy B.D., Zilla P., Franz T. Aortic valve leaflet mechanical properties facilitate diastolic valve function. *Comput Methods Biomech Biomed Engin*, 2010, vol. 13(2), 225-234.
- [21]. Kuan M.Y.S., Espino D.M. Systolic fluid-structure interaction model of the congenitally bicuspid aortic valve: assessment of modelling requirement. *Comput Methods Biomech Biomed Eng*. In Press DOI: 10.1080/10255842.2014.900663
- [22]. Lamata P., Pitcher A., Krittian S., Nordsletten D., Bissell M.M., Cassar T., Barker A.J., Markl M., Neubauer S., Smith N.P. Aortic relative pressure components derived from four-dimensional flow cardiovascular magnetic resonance. *Magn Reson Med*, 2014 vol. 72(4), 1162-1169.
- [23]. Lavdaniti M. Invasive and non-invasive methods for cardiac output measurement. *Int J Caring Sci*, 2008, vol. 1(3), 112–117.
- [24]. Lindroos M., Kupari M., Heikkilä J., Tilvis R. Prevalence of aortic valve abnormalities in the elderly: an echocardiographic study of a random population sample. *J Am Coll Cardiol*, 1993, vol. 21(5), 1220-1225.
- [25]. Lund O., Emmertsen K., Dorup I., Jensen F., Flo C. Regression of Left Ventricular Hypertrophy During 10 Years After Valve Replacement for Aortic Stenosis is Related to the Preoperative Risk Profile *Eur Heart J*, 2003, vol. 24, 1437–1446.
- [26]. Murphy S.L., Xu J. *Deaths: Preliminary Data for 2010*. 1st ed. Atlanta: National Vital Statistics Reports. 2012.
- [27]. Park S.H., Lee S.J., Kim J.Y., Kim M.J., Lee J.Y., Cho A.R., Lee H.G., Lee S.W., Shin W.Y., Jin D.K. Direct Comparison between Brachial Pressure Obtained by Oscillometric Method and Aortic Pressure Using Invasive Method. *J Soonchunhyang Medical Science*, 2011, vol. 17(2), 65-71.
- [28]. Rajappan K., Rimoldi O., Dutka D., Ariff B., Pennell D., Sheridan D., Camici P. Mechanisms of Coronary Microcirculatory Dysfunction in Patients With Aortic Stenosis and Angiographically Normal Coronary Arteries. *Circulation*. 2002, vol. 105, 470–476.

- [29]. Razminia M., Trivedi A., Molnar J., Elbzour M., Guerrero M., Salem Y., Lubell D.L. Validation of a new formula for mean arterial pressure calculation: the new formula is superior to the standard formula. *Catheter Cardiovasc Interv*, 2004, vol. 63(4), 419-425.
- [30]. Stouffer G.A. Aortic regurgitation. *Cardiovascular Hemodynamics for the Clinician*. Oxford: Wiley-Blackwell. 2008.

Tables:

Table 1. Geometric parameters of the aortic valve.

(I)	(II)	(III)	(IV)	(V)	(VI)	(VII)
Ascending aorta radius after sinotubular junction (mm)	Aortic radius (mm)	side Leaflet's thickness (mm)	Valve's height (mm)	Leaflet's length (mm)	Ventricular side radius (mm)	Maximum radius of normal aortic root (mm)
11.75	11.5	0.6	20.36	16.6	11.1	16.65

Table 2. Mechanical properties

Viscosity (Pa.s)	Density (kg/m ³)	Young's modulus (N/m ²)	Poisson ratio
3.5×10^{-3}	1056	6.8×10^6	0.49

Table 3. Hemodynamic changes to different severity of aortic stenosis.

Percentage of stenosis	Percentage of area full opening	Percentage of diameter of full opening	Increase in cardiac output over the exercise (%)	Decrease in stroke volume over the exercise (%)	Mean slope of cardiac outputs to heart rate (ml/min.bpm)	Mean slope of stroke volume changes to heart rate (ml/beat.bpm)	Mean slope of cardiac output changes to mean arterial pressure (ml/min.mmHg)	Mean slope of stroke volume changes to mean arterial pressure (ml/beat.mmHg)
0 (healthy)	100	100	60	7.1	-83	-0.100	-19.7	-0.42
20 (normal)	80	90	58.1	9.0	-65	-0.095	-15.4	-0.40
30 (mild)	70	84	58.4	9.0	-58	-0.083	-13.8	-0.35
40 (moderate)	60	78	58.7	8.1	-50	-0.072	-11.9	-0.30
50 (severe)	50	71	58	7.9	-44	-0.060	-10.4	-0.25
60 (critical)	40	63	58.4	8.1	-36	-0.052	-8.5	-0.22

Table 4. Hemodynamic changes of stenosed aortic valve to heart rate.

Heart rate (bpm)	98	106	114	125	136	147	153	159	169
Mean gradient of cardiac output	-91	-	-	-	-	-	-	-	-
changes to stenosis severity (ml/min)		100	109	116	125	135	134	140	147
Mean gradient of stroke volume	-	-	-	-	-	-	-	-	-
changes to stenosis severity (ml/beat)	0.92	0.94	0.96	0.93	0.92	0.92	0.88	0.88	0.87

ACCEPTED

Figure captions:

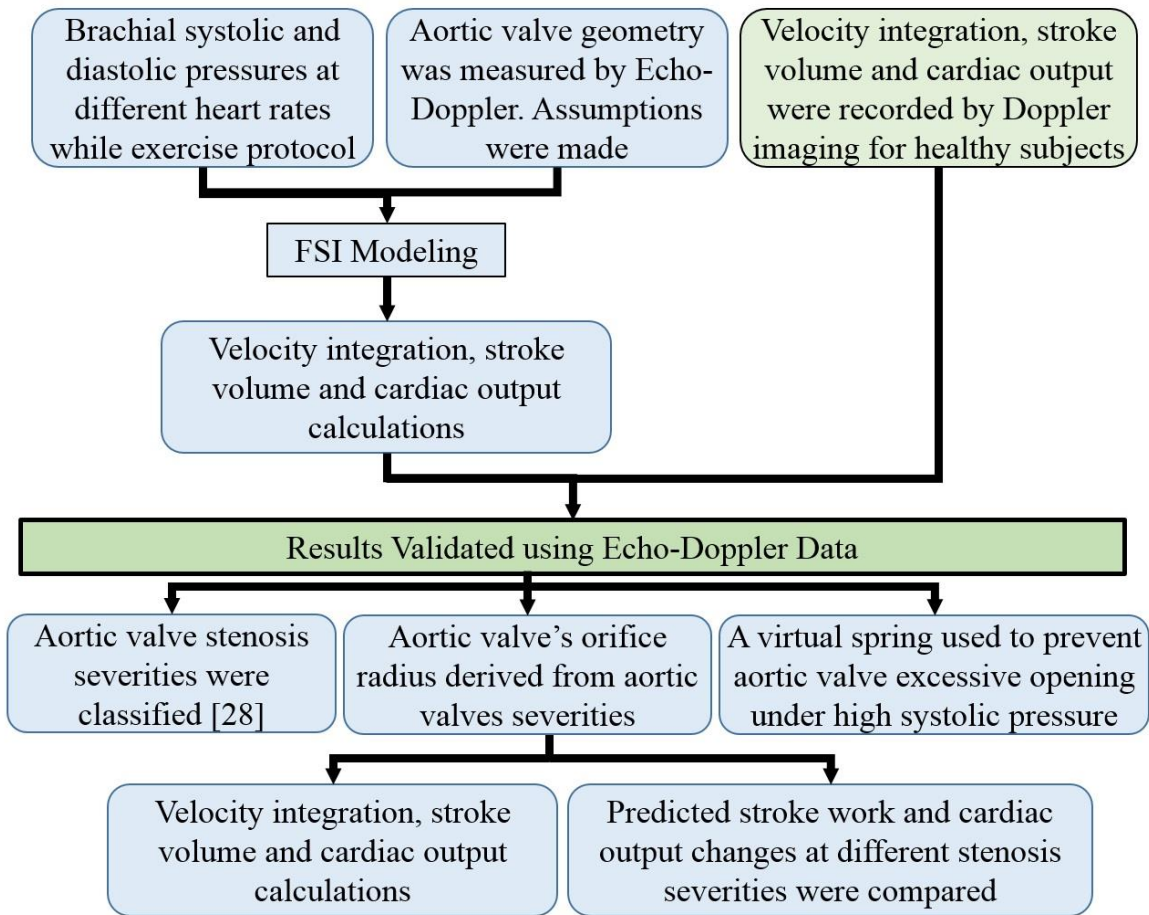


Fig. 1. Workflow

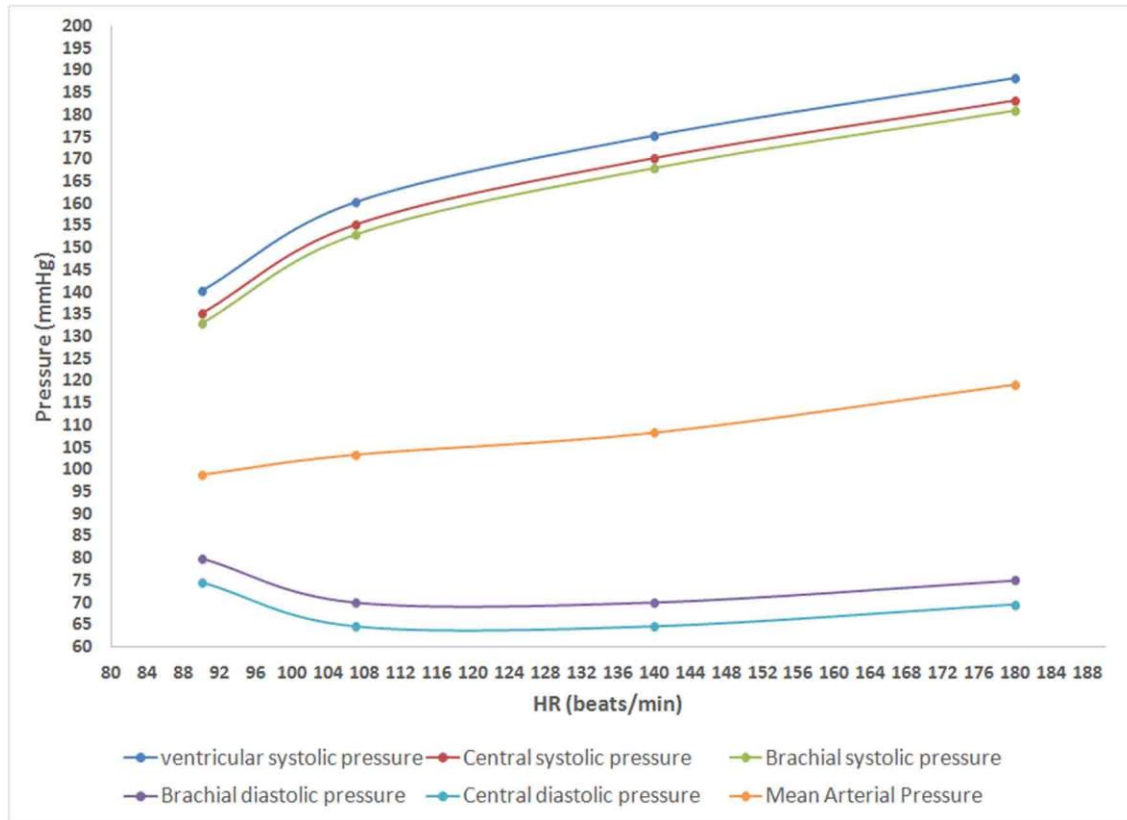


Fig. 2. (a) Interpolated curves for ventricular systolic pressure (VSP), Aortic systolic pressure (CSP), brachial systolic pressure (BSP), **(b)** brachial diastolic pressure (BDP) and Aortic diastolic pressure (CDP).

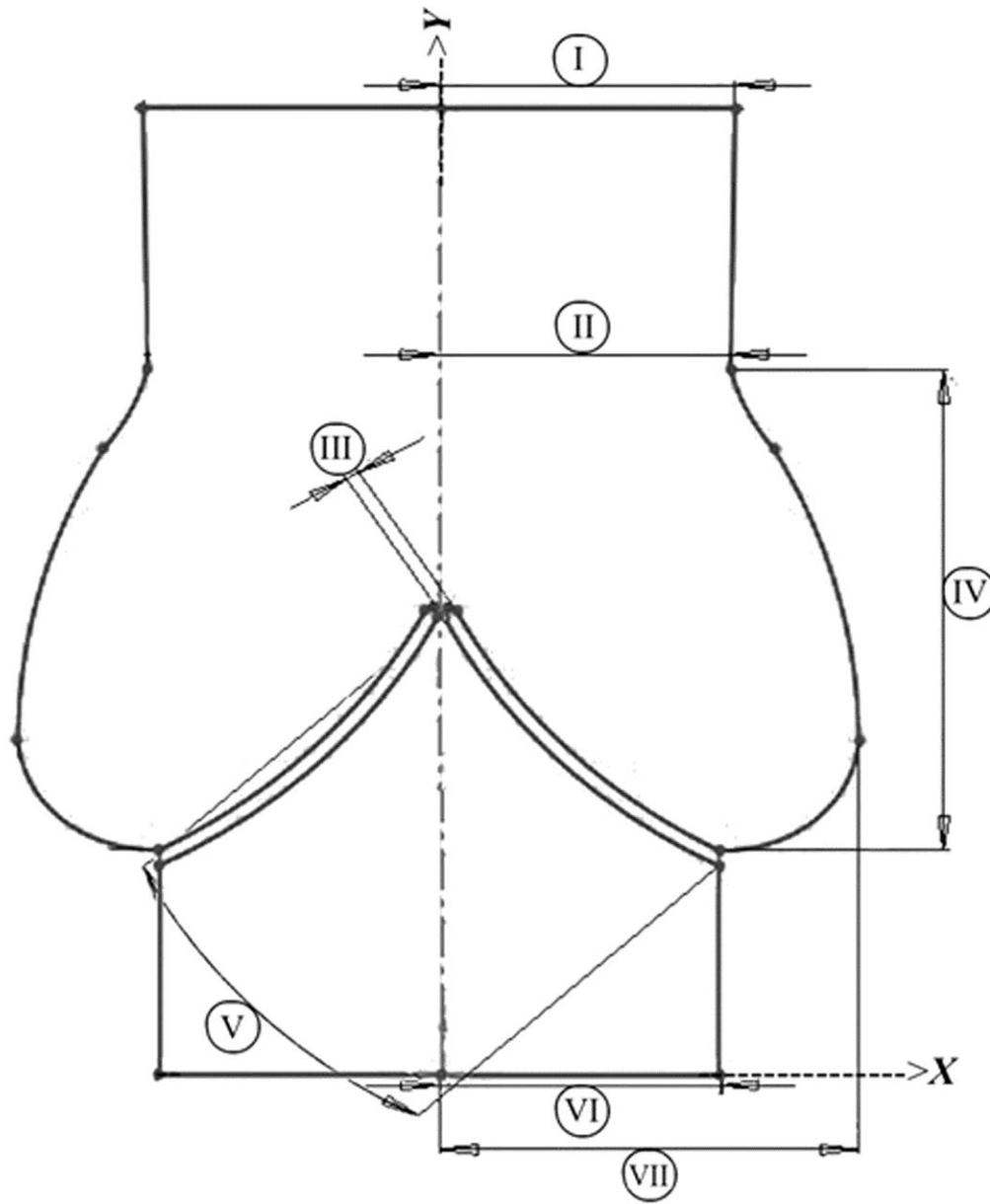


Fig. 3. I) Ascending aorta radial after sinotubular site; II) Aortic side radial; III) Leaflet thickness; IV) Valve height; V) Leaflet length; VI) Ventricular side radial; VII) Maximum radius of normal aortic root.

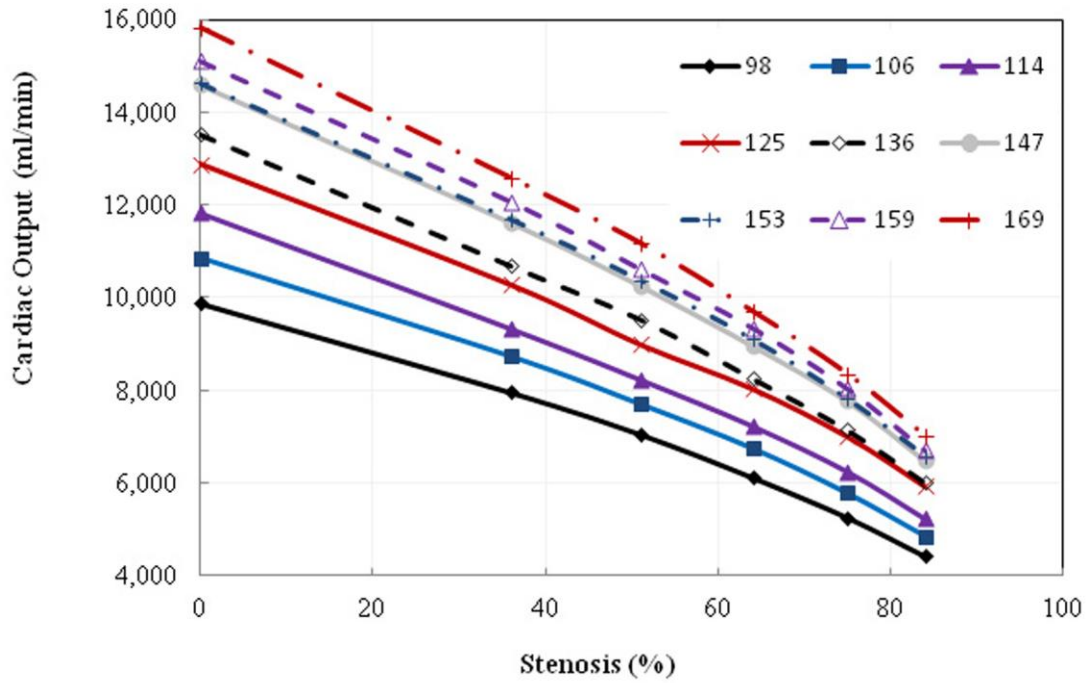


Fig. 4. FSI prediction of cardiac output changes at various severities of stenosis.

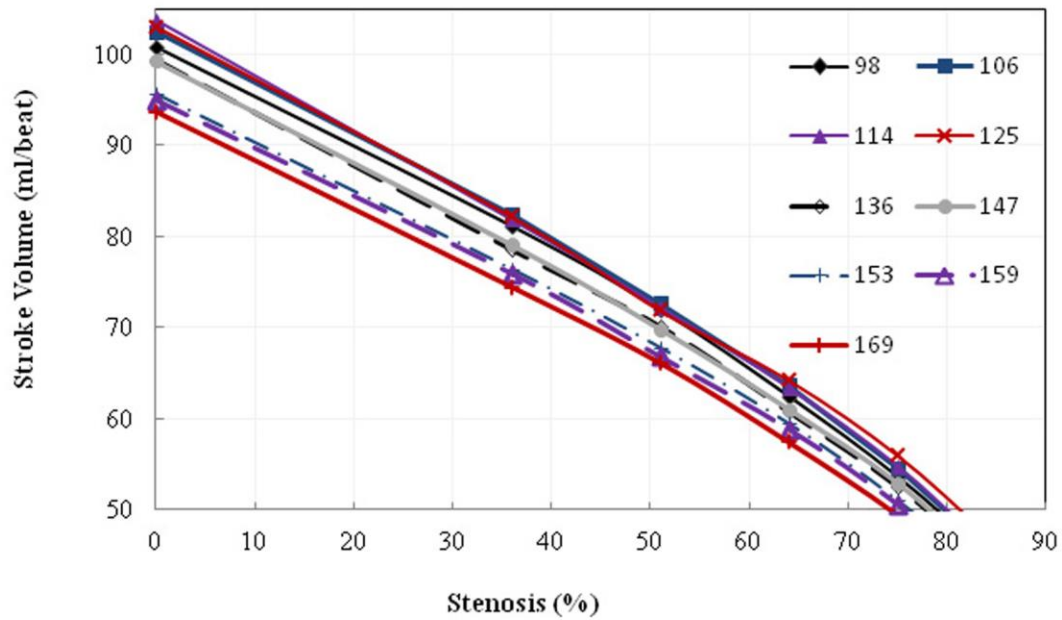


Fig. 5. FSI prediction of stroke volume changes at various severities of stenosis.

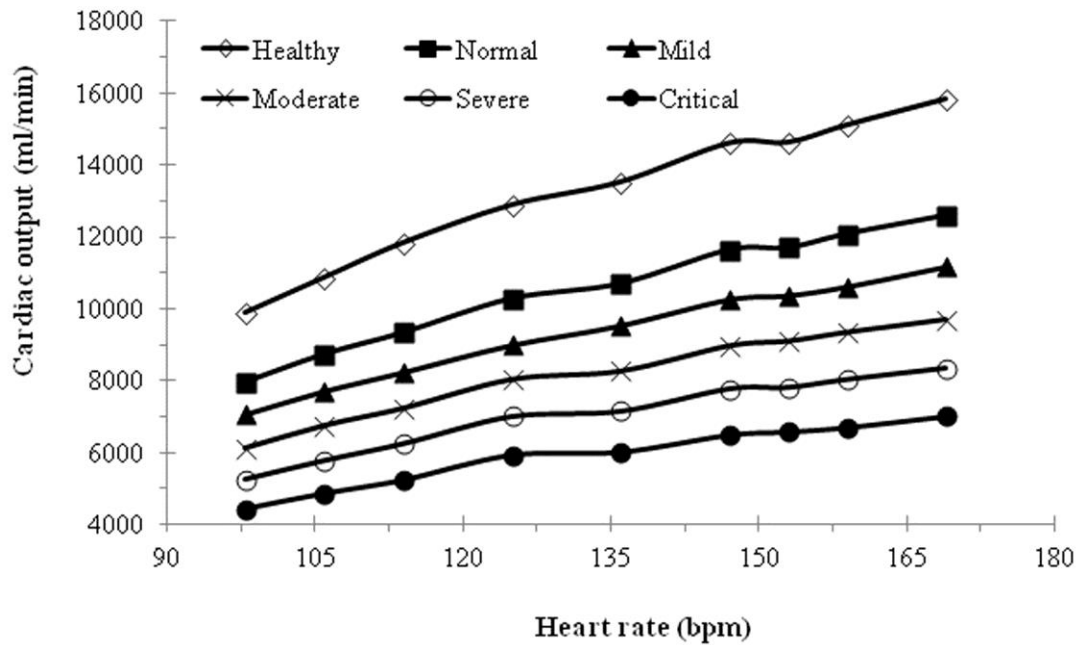


Fig. 6. FSI prediction of cardiac output changes to heart rate at different stenosis severities.

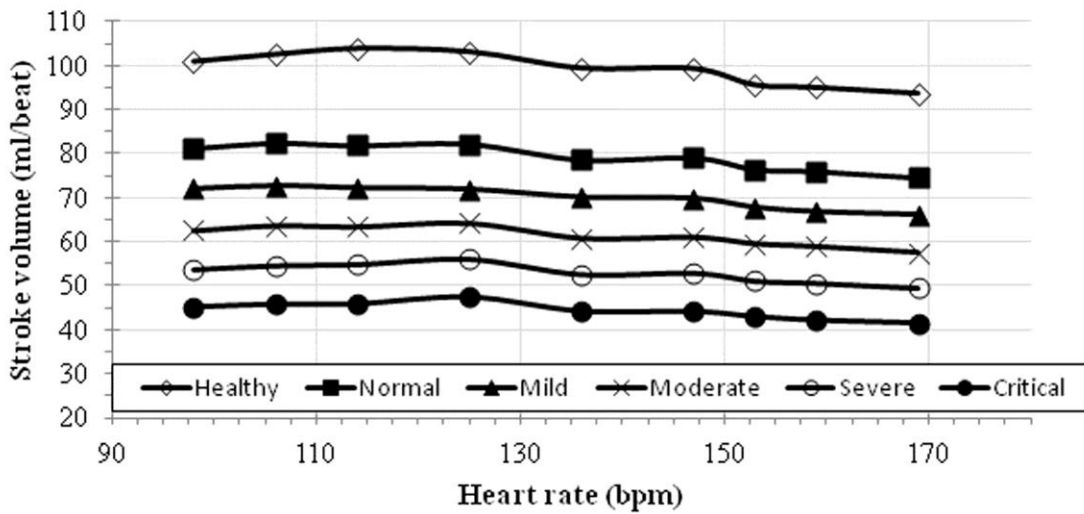


Fig. 7. FSI prediction of stroke volume changes with heart rate at different stenosis severities.

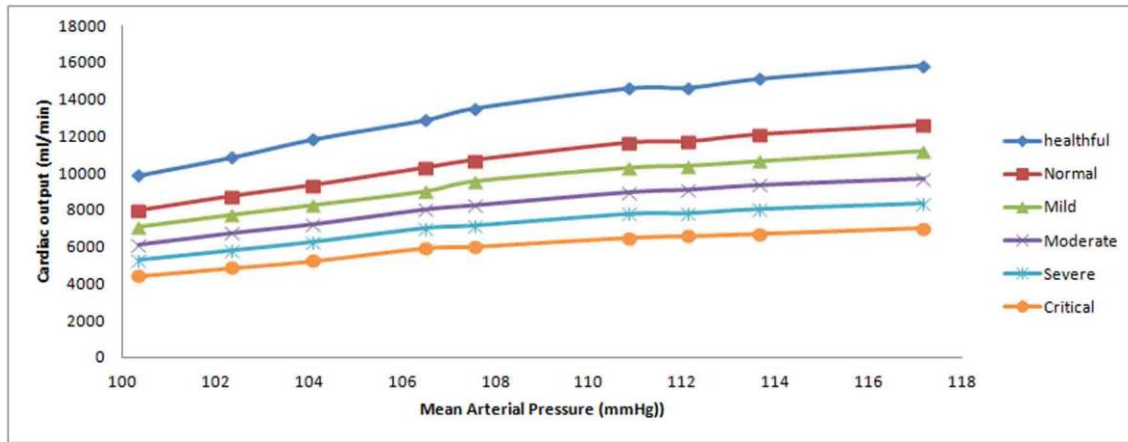


Fig. 8. FSI prediction of cardiac output changes to mean arterial pressure at different stenosis severities.

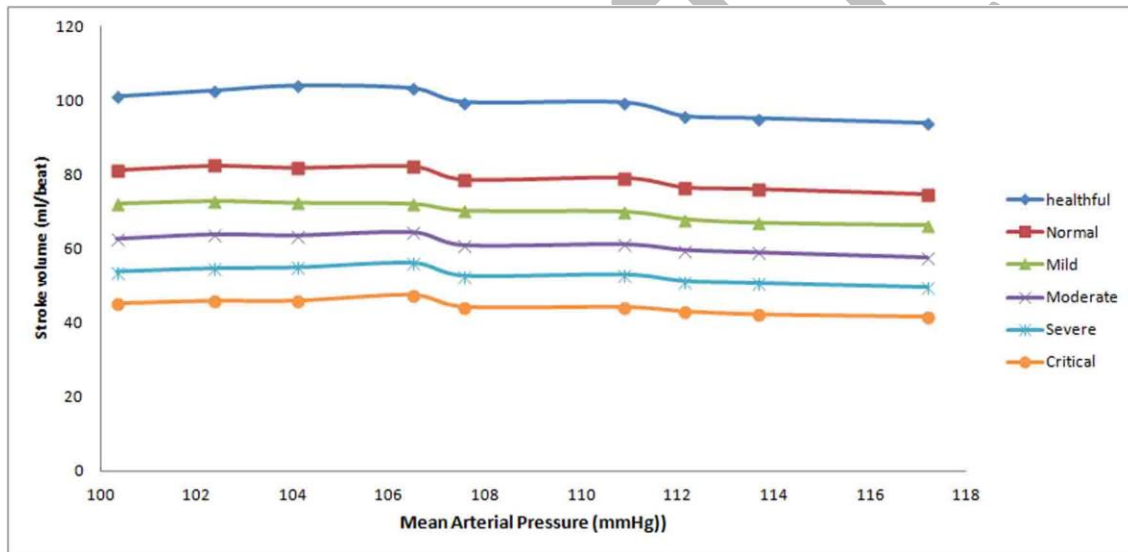


Fig. 9. FSI prediction of stroke volume changes to mean arterial pressure at different stenosis severities.